

Zero wave resistance for ships moving in shallow channels at supercritical speeds. Part 2. Improved theory and model experiment

By XUE-NONG CHEN¹, SOM DEO SHARMA²
AND NORBERT STUNTZ³

¹Institute for Nuclear and Energy Technologies, Forschungszentrum Karlsruhe, Germany

²Institute of Ship Technology and Transport Systems, Gerhard Mercator University, Duisburg, Germany

³VBD – European Development Centre for Inland and Coastal Navigation, Duisburg, Germany

(Received 2 May 2002 and in revised form 15 August 2002)

This paper deals with a specially designed slender ship moving steadily at a chosen supercritical speed in a suitable narrow shallow channel such that the wave resistance becomes zero. It is a sequel to Chen & Sharma (1997), which predicted theoretically the existence of a ship–channel configuration of zero wave resistance. It was derived from a two-soliton solution of the Kadomtsev–Petviashvili equation. The present theory comprises an improved shallow-water wave equation of Boussinesq type for the far field and an enhanced slender body approximation in the near field. Moreover, a physical model experiment performed in the Duisburg shallow water towing tank (VBD) is reported. It confirms that at the exact design condition the ship's reflected bow wave cancels the stern wave so completely that there are almost no waves behind the ship and the measured resistance is reduced so much that the wave resistance component is practically zero.

1. Introduction

In an earlier paper (Chen & Sharma 1997) two of the present authors predicted on the basis of an entirely theoretical analysis that the bow and stern waves of a slender ship moving in a narrow shallow channel at a chosen supercritical speed can be made to cancel each other so completely by a proper choice of hull–channel geometry that there are no free waves behind the ship and, accordingly, it experiences no wave resistance.

At supercritical speeds, i.e. $U > \sqrt{gh}$, where U is the ship speed, g the acceleration due to gravity and h the water depth, the ship wave pattern looks like the shock waves of a two-dimensional airfoil in supersonic flight. Both bow and stern waves extend aft obliquely along their characteristic lines. But the bow wave is essentially a free-surface elevation and the stern wave a depression, see figure 1(a). By the nature of nonlinear shallow-water waves, the elevation can form an oblique soliton through a balance of nonlinearity and dispersion, but the depression can never form a 'negative soliton' and is necessarily dispersed. If the ship moves symmetrically along the centreline of a narrow shallow channel of rectangular cross-section, its waves must be reflected by the vertical sidewalls. If, further, the hull–channel geometry is

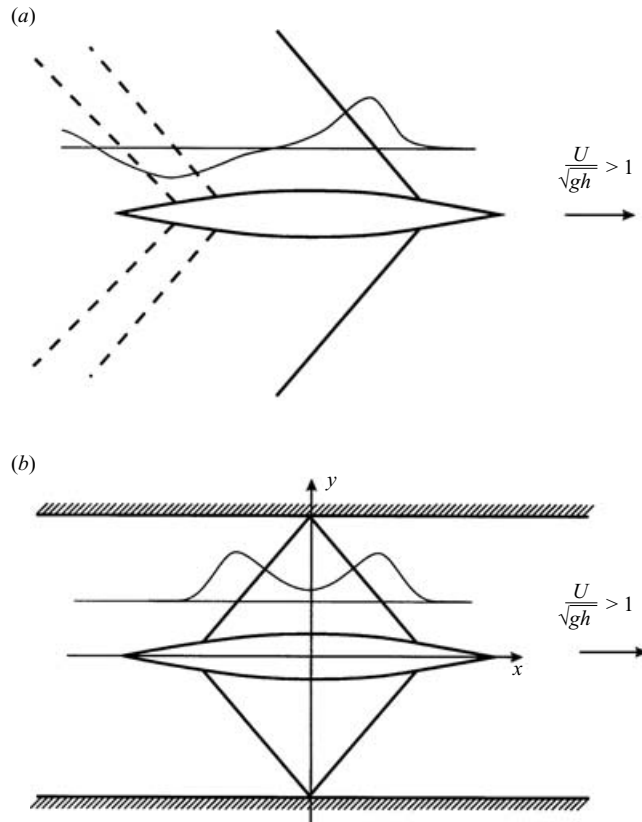


FIGURE 1. Schematic of ship wave patterns at supercritical speed; moving coordinate system. (a) In horizontally unbounded shallow water. (b) In a narrow shallow channel (design condition).

adapted to the chosen depth Froude number as required by the theory, the bow wave after reflection from the channel sidewall would hit the after-body and cancel the stern wave so that at the design speed the resultant wave in the ship's wake would disappear totally, see figure 1(b). We have previously proposed the name 'shallow channel superconductivity' for this phenomenon.

The above theoretical result was subject to the restriction of the Kadomtsev–Petviashvili (KP) shallow-water wave equation in the far field, which ignores viscosity and accounts only to a certain extent for weak nonlinearity and dispersion, and of the simple slender-body approximation in the near field, which accounts for the flow displacement effect of the ship's hull only to first order. This paper, a logical continuation of the previous one, comprises two parts, namely a theoretical and an experimental part. In the first part we attempt to improve the theory by replacing the KP equation by an equation of Boussinesq type and by extending the slender-body approximation to second order. An approximate two-soliton solution is obtained following the approach of Miles (1977). In the second part, which may be the more important, we report a model experiment carried out recently in the VBD towing tank at Duisburg for validating our theory. The experimental results are shown in detail as measured resistance curves and wave cuts, and illustrated by photographs of the wave pattern. The experiment demonstrates that in the exact design condition the ship's (reflected) bow and stern waves indeed cancel each other so completely that

almost no waves are observed behind the ship, and that the measured total resistance is reduced so far that the estimated wave resistance becomes practically zero. This is further corroborated by a comparison of measured and theoretical wave cuts.

2. Theory

2.1. Mathematical model

The particular problem considered here is a slender ship of length l , maximum beam b_m and draught d moving along the centreline of a straight rectangular shallow channel of uniform depth h and width w . A right-handed Cartesian coordinate system $Oxyz$ moving at the same speed as the ship is used with origin O located at the centre-point on the ship's waterline plane, the plane Oxy coinciding with the quiescent free surface, the axis z positive upward, and the axis x positive forward, as shown in figure 1(b). The problem is obviously symmetric about the Ozx -plane, and if the ship does not move at near-critical speeds, it can be treated as steady.

Unless otherwise stated, all variables are non-dimensionalized by reference to water depth h , the acceleration due to gravity g , and the water density ρ . The same symbols are used from now on for non-dimensional variables. For example, $l/h \rightarrow l$ is non-dimensional ship length, $S_m/h^2 \rightarrow S_m$ is non-dimensional midship section area, etc. Note that our non-dimensional speed $U/\sqrt{gh} \rightarrow U$ is usually called the depth Froude number F_{nh} .

The problem lends itself to a simplified solution by the method of matched asymptotic expansions, exploiting in a natural way the assumed shallowness of the water $h/l_W \ll 1$, where l_W is a typical wavelength, and the assumed slenderness of the ship $\sqrt{S_m}/l \ll 1$, see e.g. Mei (1976), Mei & Choi (1987), Chen & Sharma (1994) and Chen (1999). The following is an improved version of our previous mathematical model (Chen & Sharma 1997) as applied to the special case in hand.

The far-field flow is governed by a two-dimensional slowly time-varying shallow-water wave equation, Chen (1999, equation 1.40),

$$2U\varphi_{xt} + (1 - U^2)\varphi_{xx} + \varphi_{yy} + U\varphi_x\varphi_{yy} + 3U\varphi_x\varphi_{xx} + 2U\varphi_y\varphi_{xy} + \frac{1}{3}U^2(\varphi_{xxx} + \varphi_{xyy}) = 0, \quad (2.1)$$

where $\varphi(x, y, t)$ is a depth-averaged perturbation velocity potential. This is a fairly general model functioning in a wide speed range from subcritical to supercritical, explicitly including the transcritical speed range where unsteady effects such as upstream solitons are known to occur. However, for the present application to clearly supercritical speeds we need only its stationary form, i.e. the term φ_{xt} is to be dropped. Moreover, since now $U > 1$, if y is formally seen as time, the analogy to a one-dimensional Boussinesq-type equation becomes evident (Drazin & Johnson 1989). The free-surface elevation ζ can be approximated as

$$\zeta(x, y) = U\varphi_x. \quad (2.2)$$

In the near-field flow around the ship, the law of mass conservation can be exploited in terms of averaged velocities to yield an explicit boundary condition at the waterline $y = \pm b(x)/2$. Omitting the details, an improved slender-body approximation is found to be

$$\varphi_y = \mp \frac{1}{2(1 + \zeta)} \left\{ \frac{d}{dx} [(U - \varphi_x)S_f(x)] - b(x) \frac{d}{dx} [(1 + \zeta)(U - \varphi_x)] \right\} \quad \text{at } y = \pm b(x)/2, \quad (2.3)$$

where

$$S_f(x) = S_0(x) + (s + \theta x)b(x) + \zeta(x)b(x) \tag{2.4}$$

is an effective sectional area taking account of running sinkage s , running trim angle θ (positive bow downward), and local wave elevation ζ at the waterline. Since we are dealing with slender ships the waves generated are expected to be small. So we introduce a smallness parameter $\varepsilon = A/h$, where A is a typical wave amplitude. A natural normalization of equation (2.3) then yields the relation $S_m/(hl) = O(\varepsilon)$ between hull slenderness and wave smallness. By an analysis similar to Chen (1999) it can be shown that the improved boundary equation (2.3) is of $O(\varepsilon^2)$ and, hence, consistent with the improved field equation (2.1) after normalization, see equation (2.7) in the next subsection.

The formulation of the problem is completed by specifying the simple no-flux boundary condition on the channel sidewalls:

$$\varphi_y(x, \pm w/2) = 0. \tag{2.5}$$

The numerical task, especially in the inverse design problem, can be made much easier by shifting the boundary condition (2.3) from the waterline $y = \pm b(x)/2$ to the centreline $y = 0$. Using truncated Taylor series expansions,

$$\varphi_y(x, \pm \frac{1}{2}b(x)) = \varphi_y(x, \pm 0) \pm \frac{1}{2}b(x)\varphi_{yy}(x, \pm 0),$$

and dropping terms of third order, which also allows the approximation $\varphi_{yy} = (U^2 - 1)\varphi_{xx}$, a surprisingly simple form of equation (2.3) results:

$$\varphi_y(x, \pm 0) = \mp \frac{1}{2(1 + \zeta)} \left\{ \frac{d}{dx} [(U - \varphi_x)S_f(x)] \right\}. \tag{2.6}$$

This equation is given in Chen & Sharma (1994) but derived there by matched asymptotic expansions. An equation equivalent in precision to (2.3) was obtained by Chen (1999, equation 2.34) in yet another mathematical manner.

2.2. Approximate solution

As far as we know, equation (2.1) has no exact analytic two-soliton solution. But an approximate solution can be found if the two solitons propagate in sufficiently different directions, a case called the weak interaction by Miles (1977). For this purpose we exploit the already introduced formal smallness parameter $\varepsilon = A/h$ and normalize variables as follows:

$$\varphi = \sqrt{\varepsilon}\phi, \quad x = X/\sqrt{\varepsilon}, \quad y = Y/\sqrt{\varepsilon}.$$

Thus equation (2.1) becomes

$$(1 - U^2)\phi_{XX} + \phi_{YY} + \varepsilon U\phi_X\phi_{YY} + 3\varepsilon U\phi_X\phi_{XX} + 2\varepsilon U\phi_Y\phi_{XY} + \frac{1}{3}\varepsilon U^2(\phi_{XXXX} + \phi_{XXYY}) = O(\varepsilon^2). \tag{2.7}$$

Here, we consider only the supercritical case $U > 1$. Let us assume the above equation has a two-soliton solution of a form given by Miles (1977),

$$\phi = F(\xi + \varepsilon\sigma_1(\eta)) + G(\eta + \varepsilon\sigma_2(\xi)) \tag{2.8}$$

with

$$\xi = X + \cot\alpha_1 Y - X_1, \quad \eta = X + \cot\alpha_2 Y + X_2,$$

where F and G are single-soliton or solitary wave-train solutions, σ_1 and σ_2 are phase shift functions due to the two-soliton interaction, X_1 and X_2 are initial phase

constants, and α_1 and α_2 are the angles between the phase lines and the positive x -axis. It is understood that two-component solitons are propagating in directions with equal positive x -component and possibly unequal but opposite y -components, implying that $\cot \alpha_1$ and $\cot \alpha_2$ have different signs. Weak interaction in the sense of Miles is ensured if U is sufficiently larger than unity.

By substituting equation (2.8) into equation (2.7) and straightforward calculation we obtain the condition

$$\begin{aligned} & (1 - U^2 + \cot^2 \alpha_1)F_{\xi\xi} + 3U\varepsilon(1 + \cot^2 \alpha_1)F_{\xi}F_{\xi\xi} + \frac{1}{3}\varepsilon U^2(1 + \cot^2 \alpha_1)F_{\xi\xi\xi\xi} \\ & + (1 - U^2 + \cot^2 \alpha_2)G_{\eta\eta} + 3U\varepsilon(1 + \cot^2 \alpha_2)G_{\eta}G_{\eta\eta} + \frac{1}{3}\varepsilon U^2(1 + \cot^2 \alpha_2)G_{\eta\eta\eta\eta} \\ & + \varepsilon F_{\xi\xi} \left[2(1 - U^2 - \cot^2 \alpha_2)\frac{d\sigma_1}{d\eta} + U(3 - \cot^2 \alpha_2)G_{\eta} \right] \\ & + \varepsilon G_{\eta\eta} \left[2(1 - U^2 - \cot^2 \alpha_1)\frac{d\sigma_2}{d\xi} + U(3 - \cot^2 \alpha_1)F_{\xi} \right] = O(\varepsilon^2). \end{aligned}$$

Since F and G are soliton solutions, each of the first two lines in the above condition is *a priori* equal to zero. By setting each of the last two lines also equal to zero and remembering that F and G are independent and non-zero, we can solve for the free parameters σ_1 and σ_2 :

$$\sigma_1 = \frac{U(3 - \cot^2 \alpha_2)}{2(U^2 + \cot^2 \alpha_2 - 1)}G(\eta), \tag{2.9}$$

$$\sigma_2 = \frac{U(3 - \cot^2 \alpha_1)}{2(U^2 + \cot^2 \alpha_1 - 1)}F(\xi). \tag{2.10}$$

In other words, with σ_1 and σ_2 chosen as above, equation (2.8) becomes a solution of equation (2.7), correct to $O(\varepsilon)$. We now choose the following particular single-soliton solutions F and G :

$$\begin{aligned} F(\xi) &= A_1/k_1 \tanh(k_1\xi), & G(\eta) &= A_2/k_2 \tanh(k_2\eta), \\ \cot^2 \alpha_i &= \frac{U^2}{1 + A_i U} - 1, & k_i &= \frac{\sqrt{3A_i U}}{2U}, \quad i = 1, 2, \end{aligned}$$

where A_i is the soliton amplitude and k_i is its wavenumber. To ensure symmetry about the plane $y = w/2$, which is physically equivalent to satisfying the no-flux boundary condition on the channel sidewall, we have to set $A_1 = A_2 = A$, $k_1 = k_2 = k$, $x_1 = x_2 = x_0$, $\cot \alpha_1 = -\cot \alpha_2 = \cot \alpha$, subject to the conditions

$$\begin{aligned} \cot \alpha &= \sqrt{(U^2 - 1 - AU)/(1 + AU)}, \\ k &= \frac{\sqrt{3AU}}{2U}, \\ w &= 2x_0/\cot \alpha. \end{aligned}$$

This solution represents a twin soliton, a particularly simple configuration possessing yet another symmetry, namely about the y -axis, which, however, is not a necessary condition for obtaining zero wave resistance, see Chen & Sharma (1996).

In order to check and possibly improve the precision of this approximate solution, we performed a test study by means of the stationary standard KP equation for which both exact and approximate solutions exist. The comparison showed that phase-shift functions somewhat similar to (2.9) and (2.10) describe the process quite well but not its final asymptotic value. The approximate solution underestimates the asymptotic

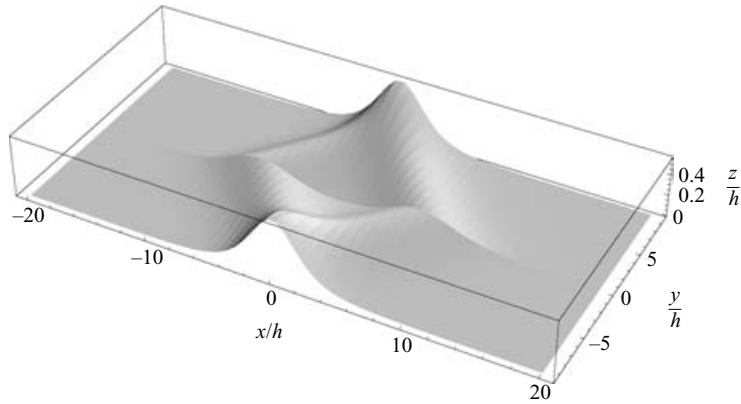


FIGURE 2. Theoretical ship wave pattern at the design condition; the ship is at the centreplane $y = 0$, channel sidewalls are at $y/h = \pm 9.5$.

phase shift by more than 50% for the design value of A . This suggested a heuristic improvement of the approximate solution by introducing in front of the phase function a constant factor f_c , which can be easily estimated as the ratio of the asymptotic phase shifts in the two KP solutions. It worked very well for the KP equation and encouraged us to apply it to the present approximate solution using a value of the factor derived for a KP equation of identical parameter values. Equation (2.8), thus modified, reads

$$\phi = F(\xi + \varepsilon f_c \sigma_1(\eta)) + G(\eta + \varepsilon f_c \sigma_2(\xi)), \quad (2.11)$$

with $f_c = 2.3$ for the design condition $U = 1.414$, $\varepsilon = A/h = 0.15$ and $x_0 = X_0/\sqrt{\varepsilon} = 7.65636$, defined in the next section. The theoretical wave pattern for this condition is shown in figure 2. (See the Addendum for a further discussion of the phase-shift factor f_c .)

3. Design

The design task consists of two steps. First, the cross-sectional area curve of the ship and the appropriate channel width are determined by theory for a chosen depth Froude number and a trial twin-soliton, requiring some iteration to achieve a prescribed hull displacement. Second, the detailed section shape, not prescribed by the theory, is selected to meet the practical demand of a fair and simple hull geometry. Also for simplicity, a ‘fixed’ towing mode is assumed, i.e. no running sinkage and trim are permitted. This is not an inherent limitation imposed by the theory, but it does facilitate the design of the experiment by precluding possible differences between the theoretical and real values of sinkage and trim in the ‘free’ towing mode. The running trim, by the way, is always zero in theory for a fore-and-aft symmetric hull form in the waveless state.

In principle, three non-dimensional parameters, x_0 , A and U , can be freely chosen. The theory would then yield a non-dimensional hull-channel configuration, i.e. a family of geosims with the property of being waveless at the design Froude number U . In practice, the physical model experiment has to be conducted on an object of given absolute size. The VBD towing tank available to us is 200 m long, 9.8 m wide and 1.3 m deep. The water depth is varied easily and routinely by pumping water into

another tank, while the width can be varied on demand by erecting a temporary intermediate wall with considerable yet justifiable effort. (It suffices to erect the intermediate wall over the middle 80 m of the tank length where measurements are taken, leaving the run-in and roll-out stretches of the tank undivided.) Since it was known from previous trials that promising depth Froude numbers were around 1.5 and the ratio of channel width to ship length around 0.5, we arbitrarily specified $U = \sqrt{2}$, along with $h = 0.2$ m to ensure a feasible towing speed, and $w = 3.8$ m to ensure a reasonable model length. With absolute size and two non-dimensional parameters, namely U and w/h , now fixed, we were still free to manipulate the pair A and x_0 to obtain any desired hull displacement within a certain range. We finally chose $A = 0.15$ and $x_0 = 7.656$ as a compromise between extreme hull slenderness and excessive wave steepness.

The effective sectional area curve $S_f(x)$ can be obtained by integrating equation (2.6):

$$S_f(x) = -\frac{2}{U - \varphi_x} \int_{-\infty}^x \varphi_y(1 + \zeta) dx, \quad y = +0. \quad (3.1)$$

However, in order to obtain the nominal sectional area curve $S_0(x)$ from equation (2.4), we need to prescribe the local beam $b(x)$ at the waterline. Partly anticipating the later determination of section shapes on practical grounds, we assume a uniform draught d and a uniform sectional area coefficient C_M over the entire hull length. It follows immediately that

$$b(x) = \frac{S_0(x)}{C_M d}. \quad (3.2)$$

Substituting this into equation (2.4) we obtain easily

$$S_0(x) = S_f(x) \left[1 + \frac{\zeta(x, +0)}{C_M d} \right]^{-1}. \quad (3.3)$$

Returning now to the design of section shapes, we ensure fair waterlines by declaring all sections to be affine transforms and, hence, defined by a single non-dimensional function

$$y' = f(z'), \quad z' \in [-1, 0],$$

where $y' = 2y/b(x)$ and $z' = z/d$. Further, we ensure mathematical simplicity by arbitrarily choosing an exponential function

$$f(z') = \frac{1 - \exp[-7.5(z' + 1)]}{1 - \exp[-7.5]},$$

which can be integrated in closed form to yield a uniform sectional-area coefficient

$$C_M = \int_{-1}^0 f(z') dz' = 0.8672.$$

Now, we can either freely choose uniform draught d and determine maximum beam b_m to comply with equation (3.2) or vice versa. Our specific choice was a draught $d = 15$ cm.

One final detail remains to be explained. The theoretical sectional-area curve $S_f(x)$ extends from minus infinity to plus infinity, implying an unrealistic ship of infinite length. Luckily, the curve decays exponentially so that an approximate practical hull form of finite length can be acquired by simple truncation of the bow and stern cusps. In absolute terms, we decided upon a ship length of 6 m, leaving the stem and

Item	Symbol	Value	Unit
Length at waterline	l	6.000	m
Beam at midship	b_m	0.3892	m
Draught	d	0.150	m
Area of midship section	S_m	0.05063	m ²
Displacement volume	V	0.1283	m ³
Displacement weight	$W = \rho g V$	128	kgf
Wetted surface area	S_w	2.437	m ²
Block coefficient	$C_B = V/lb_m d$	0.3663	
Midship section coefficient	$C_M = S_m/b_m d$	0.8672	
Wetted surface coefficient	$C_{WS} = S_w/\sqrt{Vl}$	2.7776	
Length/Depth	l/h	30	
Draught/Depth	d/h	0.75	
Design speed	U	1.9803	m s ⁻¹
Design depth Froude number	$F_{nh} = U/\sqrt{gh}$	1.414	
Design water depth	h	0.200	m
Design channel width	w	3.800	m
Width/Depth	w/h	19	

TABLE 1. Principal dimensions of the ship model and the channel

stern as sharp edges of 2.7 mm thickness. The principal dimensions of final design are compiled in table 1.

Note that for the same values of parameters U , A/h and x_0 as above a hull form designed according to our original recipe (Chen & Sharma 1997) would have about 45% more displacement than the present form. This difference accrues from a more accurate treatment of wave nonlinearity and of effective hull sectional area in the present approach. (We note in passing that since the original design was never validated by physical experiment, it is hard to say exactly just how much less efficient it would have been. In other words, the gain in accuracy effected by improvement of the theory cannot be quantified on the basis of the evidence available.)

4. Model experiment

To verify the foregoing theory an experiment was carried out in the VBD towing tank. As stated above, the ship model was towed in the fixed mode. Resistance and wave cuts were recorded not only in the design narrow channel of 3.8 m width but also in the undivided towing tank of 9.8 m width. The latter is large enough to simulate effectively sidewise unrestricted water and, hence, to serve as a reference.

Figure 3 shows our main result, namely the curves of specific total resistance R_T/W measured in the narrow channel of design width (solid line connecting dots) and in the undivided tank of full width (dashed line connecting circles), both at the same design depth. For the purpose of estimating wave resistance, which unfortunately cannot be measured directly, a curve of specific frictional resistance R_F/W derived from the empirical formula of Hughes (1952, 1954) is also included. It is believed to be the best approximation of the true friction line for infinitely thin smooth plates in fully turbulent two-dimensional flow. As theoretically predicted, the measured total resistance in the narrow channel drops dramatically at the exact design speed, whereas in the wide tank the curve is as expected. Quantitatively, at the design depth Froude number 1.414 the total specific resistance in the narrow channel is 0.0102 compared to 0.0327 in the wide tank, i.e. 69% less. At the same speed, the specific

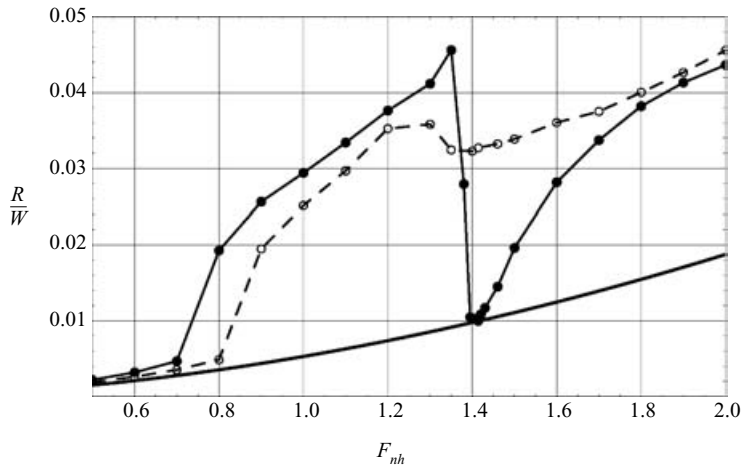


FIGURE 3. Measured specific total resistance in the narrow design channel (solid line connecting dots) and in an effectively infinitely wide channel of the same depth (dashed line connecting circles); the lowest smooth curve represents specific frictional resistance after Hughes (1952, 1954).

frictional resistance is 0.00994 after Hughes. Consequently, the residuary resistance ($R_R = R_T - R_F$) based on the Hughes line is reduced by 99%. It is reasonable to state that the wave resistance vanishes in the design condition.

Certain other features of the curves shown in figure 3 are also worth noting. First, real ship resistance curves in a finite-width shallow channel exhibit a finite transcritical speed range rather than a discrete critical speed; within the transcritical range no steady state is ever achieved even at constant ship speed, so the points shown here represent mean values, and such mean resistance curves are continuous functions of speed. These important details are missed by strictly linear wave theories but predicted well by our nonlinear wave model. Second, in the narrow channel the steep rise in resistance begins at a lower subcritical speed and the transcritical resistance plateau is accordingly higher and broader than in the wide tank. All this can be physically understood as a consequence of the stronger blockage caused by the same hull in the much smaller cross-section of the narrow channel. However, at a sufficiently high supercritical speed, when the divergence angle of the bow wave attains the appropriate value, favourable interference between the bow wave reflected from the channel sidewall and the stern wave begins to dominate, causing the two resistance curves to cross. At still higher speeds the divergence angle of the bow wave decreases again, the favourable interference dwindles, and the two resistance curves finally merge. In other words, some reduction in wave resistance can always be achieved if ship length and speed are in the correct relation to channel depth and width. This is roughly the case when $0.5 < (w/l)\sqrt{F_{nh}^2 - 1} < 1$. However, to our knowledge the total elimination of wave resistance enabled by our theoretical design has never been observed before.

Longitudinal cuts through the wave pattern were acquired by taking time records of the free-surface elevation by means of stationary wave probes as the model passed at constant speed. An array of six equidistant probes was installed along a line normal to the tank centreplane. Measurements were carried out at several speeds both in the design configuration and the reference configuration. Five of the six transverse

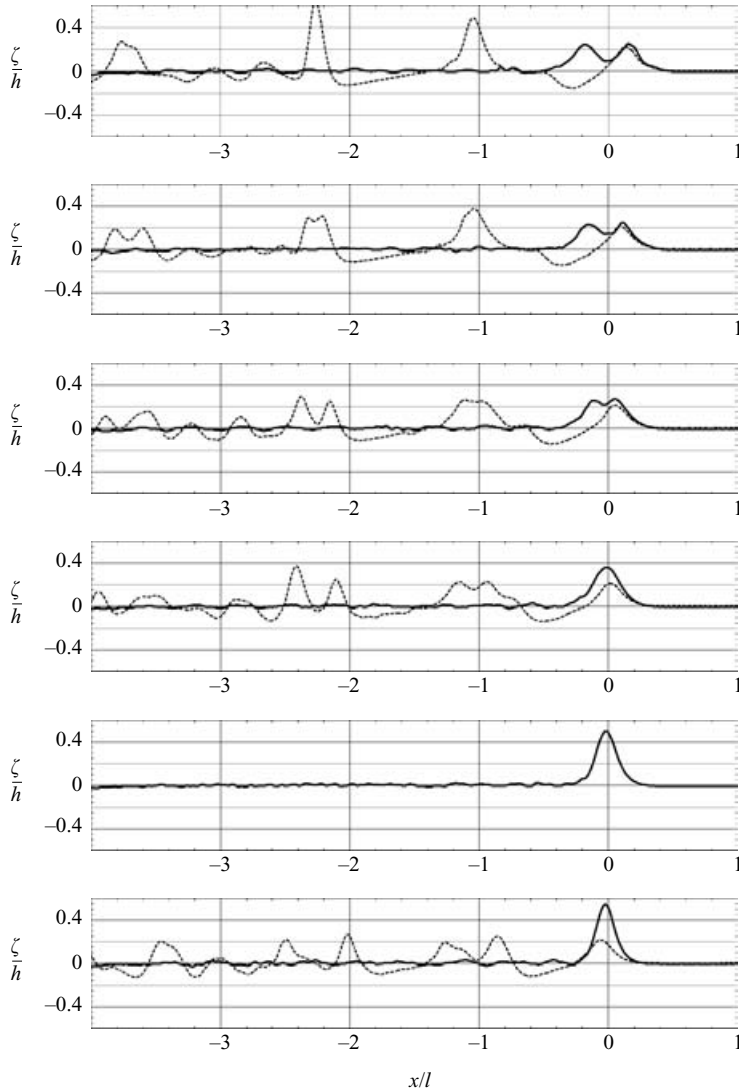


FIGURE 4. Measured wave cuts at the design depth Froude number $F_{nh} = 1.414$ ($h = 0.2$ m and $U = 1.98$ m s $^{-1}$) in the 9.8 m wide tank (dashed lines) and the 3.8 m narrow channel (solid lines); graphs from top to bottom are at $y = 0.3, 0.6, 0.9, 1.2, 1.5$ and 1.8 m. Note that the probe at $y = 1.5$ m was missing in the wide tank.

locations with respect to the model centreplane were identical in both configurations. The comparison of primary interest is, of course, at the design depth Froude number, as shown in figure 4. Evidently, the strong free waves behind the model in the wide tank are almost totally absent in the narrow design channel, in accordance with the dramatic drop in wave resistance. Quantitatively, the highest free-wave amplitude observed in the wide tank is 100 mm and in the narrow channel only 4 mm.

The most direct test of the theory is to compare the theoretical and experimental wave patterns at the design condition. This is shown in figure 5 for six equidistant longitudinal cuts. There is satisfactory agreement between theory and experiment, except for a small phase shift which may be due to bottom friction or imperfect

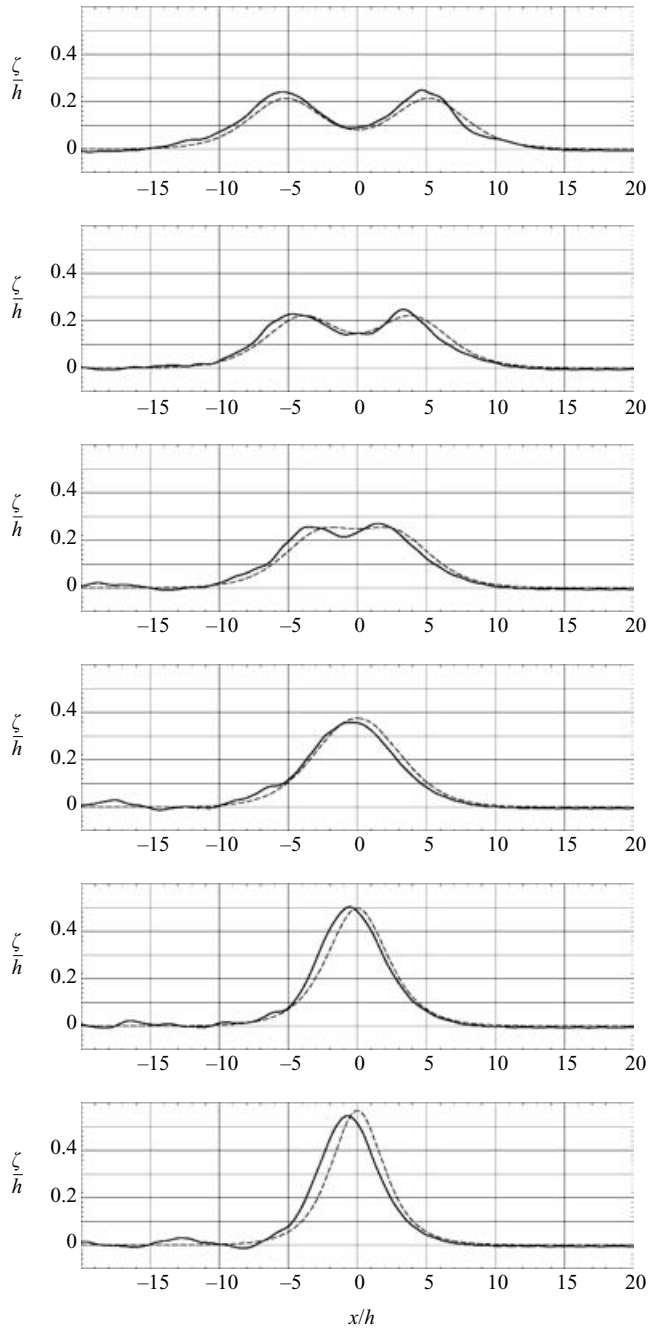


FIGURE 5. Comparison of theoretical (dashed lines) and experimental (solid lines) wave cuts at design depth Froude number $U = 1.414$ in the design narrow channel ($w/h = 19$); graphs from top to bottom are at $y/h = 1.5, 3.0, 4.5, 6.0, 7.5$ and 9.0 .

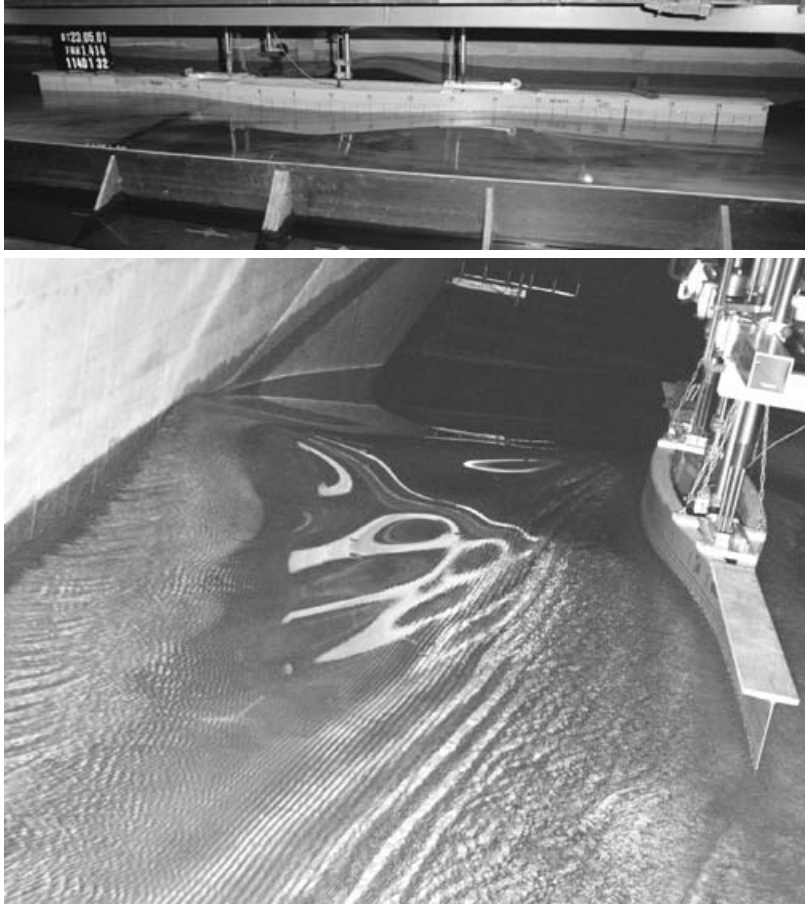


FIGURE 6. Two photographs of the wave pattern at the design condition of zero wave resistance: side view from starboard location (top) and port view from astern location (bottom).

reflection from the sidewalls. Figure 6 is an attempt to convey a visual impression of the wave pattern in the design condition of zero wave resistance. Note the two high wave crests alongside the model merging into a single crest at the channel sidewall. By contrast, the free surface behind the model is almost flat except for wake turbulence.

5. Conclusions

The theoretical prediction of a state of zero wave resistance and no trailing waves for a ship of sectional-area curve derived from a twin-soliton solution, moving at a chosen supercritical speed in a rectangular channel of appropriate depth and width has been verified by model experiments conducted in a specially designed narrow shallow channel. It is expected that the improved mathematical model presented here is more generally valid for calculating ship waves and wave resistance in shallow water.

We thank the VBD management and staff for their substantial support in conducting the model experiments in the shallow-water towing tank at Duisburg. We are also

grateful to Professor K. Kirchgässner, University of Stuttgart, for his valuable advice and encouragement.

Addendum

During the review of this paper we were asked by one of the referees to further justify the phase shift factor f_c introduced heuristically in §2.2. This led to our discovering the following approximate two-soliton solution of our Boussinesq-type equation, which is the steady version of equation (2.1), namely

$$\varphi_{yy} - (U^2 - 1)\varphi_{xx} + U\varphi_x\varphi_{yy} + 3U\varphi_x\varphi_{xx} + 2U\varphi_y\varphi_{xy} + \frac{1}{3}U^2(\varphi_{xxx} + \varphi_{xyy}) = 0. \quad (\text{A } 1)$$

This equation is conservative, i.e. it obeys at least two conservation laws. The first represents conservation of mass, as becomes evident if we rewrite the equation as follows:

$$\frac{\partial}{\partial y} [(1 + U\varphi_x)\varphi_y] = \frac{\partial}{\partial x} [(U^2 - 1)\varphi_x - \frac{3}{2}U\varphi_x^2 - \frac{1}{2}U\varphi_y^2 + \frac{1}{3}U^2(\varphi_{xxx} + \varphi_{xyy})].$$

Since φ_x , φ_y and their higher derivatives tend to zero as $x \rightarrow \pm\infty$, it yields

$$\int_{-\infty}^{\infty} (1 + U\varphi_x)\varphi_y dx = \text{constant}. \quad (\text{A } 2)$$

The integrand $F_1 = (1 + U\varphi_x)\varphi_y$ is a conserved density. Physically, it is the local (non-dimensional) mass flux in the y -direction since $1 + U\varphi_x = 1 + \zeta$ is the local water depth. The second conservation law represents conservation of momentum. It can be obtained directly by a Lagrangian formulation of equation (A 1) if y is seen as a time-like variable. The corresponding conserved density is the local (non-dimensional) momentum flux in the y -direction, namely

$$F_2 = \frac{1}{2}(1 + U\varphi_x)\varphi_y^2 + \frac{1}{2}(U^2 - 1)\varphi_x^2 - \frac{1}{2}U\varphi_x^3 - \frac{1}{6}U^2\varphi_{xy}^2 + \frac{1}{6}U^2\varphi_{xx}^2. \quad (\text{A } 3)$$

This can be confirmed by a straightforward calculation, i.e. multiplying equation (A 1) by φ_y . If we rewrite it as

$$\begin{aligned} & \frac{\partial}{\partial y} \left[\frac{1}{2}(1 + U\varphi_x)\varphi_y^2 + \frac{1}{2}(U^2 - 1)\varphi_x^2 - \frac{1}{2}U\varphi_x^3 - \frac{1}{6}U^2\varphi_{xy}^2 + \frac{1}{6}U^2\varphi_{xx}^2 \right] \\ &= \frac{\partial}{\partial x} \left[-\frac{1}{2}U\varphi_y^3 + (U^2 - 1)(\varphi_x\varphi_y) - \frac{3}{2}U\varphi_x^2\varphi_y - \frac{1}{3}U^2(\varphi_{xxx}\varphi_y + \varphi_{yyx}\varphi_y - \varphi_{xx}\varphi_{xy}) \right], \end{aligned}$$

we obtain the second conservation law

$$\int_{-\infty}^{\infty} F_2 dx = \text{constant}. \quad (\text{A } 4)$$

Now we can apply this law to determine an optimum value of the phase-shift factor f_c in (2.11). (We note in passing that the first conservation law is automatically satisfied.) If we substitute the trial solution (2.11) into expression (A 3) the x -integral of the y -derivative of F_2 should be ideally zero at any value of y . This condition can be exploited to determine an optimal value of f_c in the least-squares sense. For this we choose a number of discrete values of y in the interval $0 \leq y \leq w$ and minimize the sum

$$\sum_i \left[\int_{-\infty}^{\infty} \frac{\partial}{\partial y} F_2(x, y_i, f_c) dx \right]^2.$$

For our design parameter values the numerical solution turns out to be $f_c = 2.04$. This compares well with a similar numerical solution 2.25 that can be derived using the steady KP equation (3.1) from Chen & Sharma (1997).

The design tested and reported in this paper employed the value $f_c = 2.32$ which was not only derived from the KP equation as an approximation but also was the asymptotic rather than the numerically optimized value. We have confirmed that the exact KP solution is almost identical to the approximate solution using f_c . The use of the phase-shift factor f_c surely constitutes an improvement of the approximate solution. But surprisingly, it does not seem to affect the design channel width w .

REFERENCES

- CHEN, X.-N. 1999 Hydrodynamics of wave-making in shallow water. Doctoral Dissertation, University of Stuttgart; Shaker Verlag.
- CHEN, X.-N. & SHARMA, S. D. 1994 Nonlinear theory of asymmetric motion of a slender ship in a shallow channel. *20th Symp. on Naval Hydrodynamics, Santa Barbara, CA* (ed. E. P. Rood), pp. 386–407. US Office of Naval Research.
- CHEN, X.-N. & SHARMA, S. D. 1996 On ships at supercritical speeds. *21st Symp. on Naval Hydrodynamics, Trondheim, Norway* (ed. E. P. Rood), pp. 715–726. US Office of Naval Research.
- CHEN, X.-N. & SHARMA, S. D. 1997 Zero wave resistance for ships moving in shallow channels at supercritical speeds. *J. Fluid Mech.* **335**, 305–321.
- DRAZIN, P. G. & JOHNSON, R. S. 1989 *Solitons: an Introduction*. Cambridge University Press.
- HUGHES, G. 1952 Frictional resistance of smooth plane surfaces in turbulent flow. *Trans. Inst. Naval Archit.* **94**.
- HUGHES, G. 1954 Friction and form resistance in turbulent flow and a proposed formulation for use in model and ship correlation. *Trans. Inst. Naval Archit.* **96**.
- MEI, C. C. 1976 Flow around a thin body moving in shallow water. *J. Fluid Mech.* **77**, 737–752.
- MEI, C. C. & CHOI, H. S. 1987 Forces on a slender ship advancing in a shallow channel. *J. Fluid Mech.* **179**, 59–76.
- MILES, J. W. 1977 Obliquely interacting solitary waves. *J. Fluid Mech.* **79**, 157–169.